RESEARCH PAPER

Acta Neurobiol Exp 2023, 83: 359–376
DOI: 10.55782/ane-2023-2463

The less complex temporal patterns of resting-state EEG activity, the lower the visual temporal order threshold

Monika Lewandowska[1]*, Krzysztof Tołpa[1], Marcin Hajnowski[2], Tomasz Piotrowski[3], Joanna Dreszer[1]

[1] Department of Clinical Psychology and Neuropsychology, Institute of Psychology, Faculty of Philosophy and Social Sciences, Nicolaus Copernicus University in Torun, Toruń, Poland,
[2] Centre for Modern Interdisciplinary Technologies, Nicolaus Copernicus University in Torun, Toruń, Poland,
[3] Institute of Engineering and Technology, Faculty of Physics, Astronomy and Informatics, Nicolaus Copernicus University in Torun, Toruń, Poland,
** Email: mlewando@umk.pl*

Speech understanding, watching a movie, listening to music etc., requires perception of the temporal order of at least two incoming events. A history of performing these tasks may be reflected in spontaneous brain activity. Here, we examined the relationship between the complexity (temporal dynamics) of resting-state EEG (rsEEG) signal, assessed using the multivariate MultiScale Entropy (mMSE) algorithm, and the perception of event ordering, indexed by a visual temporal order threshold (TOT), i.e., the minimum duration necessary to correctly identify the before-after relation between two stimuli. Healthy adolescents and young adults performed a psychophysical task measuring the TOT and underwent an eyes-closed rsEEG study. The features of mMSE vectors, namely the area under curve (AUC) that represents total signal complexity, as well as the MaxSlope and the AvgEnt, corresponding to the entropy at fine- and coarse-grained timescales, respectively, were obtained for the central (midline), anterior, middle and posterior channel sets. The greater the AUC and AvgEnt values in the central, left and right posterior areas, and the higher AUC in the right middle region, the higher the TOT. The most significant relationships were found for the midline electrodes (Fz, Cz, Pz, Oz). There were no significant correlations between the MaxSlope values and the TOT. To the best of our knowledge, this is the first study demonstrating that spontaneous EEG signal complexity is associated with the temporal order perception of two stimuli presented in rapid succession. Our findings may indicate that low total and coarse entropy levels of rsEEG signal are beneficial for visual temporal order judgments.

Key words: visual temporal order threshold, resting-state EEG complexity, multivariate MultiScale Entropy

INTRODUCTION

The identification of temporal order (TO) of two sensory events that are separated by the millisecond intervals, is considered essential for cognitive processing (Fraisse, 1984; Pöppel, 1994; Mauk and Buonomano, 2004; Szelag et al., 2004; Pöppel et al., 2011). More accurate TO judgments are associated with better performance in tasks measuring fluid intelligence (Helmbold et al., 2007; Rammsayer and Brandler, 2007; Ulbrich et al., 2009; Der and Deary, 2017; Pahud et al., 2018), attention (Szymaszek et al., 2009; Ulbrich et al., 2009) and working memory (Ulbrich et al., 2009; Thomas et al., 2015; Jablonska et al., 2020). Deficits in TO perception were found in elderly people (Fitzgibbons and Gordon-Salant, 2004; Kolodziejczyk and Szelag, 2008; Szymaszek et al., 2009), language-disordered populations (Tallal et al., 1996; von Steinbüchel et al., 1999; Rey et al., 2002; Fink et al., 2006a; Szelag et al., 2014) and patients with visuospatial neglect (Eramudugolla et al., 2007; Sinnett et al., 2007).

Received 23 December 2022, accepted 8 September 2023

An ability to determine TO is usually assessed in laboratory conditions using the temporal order threshold (TOT), which is defined as the minimal inter-stimulus interval (ISI) between two consecutive sensory events necessary to identify their before-after relation (Wittmann and Szelag, 2003; Fink et al., 2006b; Szymaszek et al., 2009; Ulbrich et al., 2009; Szelag et al., 2018; Jablonska et al., 2020; Lewandowska et al., 2022). The TOT values in healthy young adults are between 20 and 60 msec, regardless of the sensory modality (Hirsh and Sherrick, 1961; Swisher and Hirsh, 1972; Kanabus et al., 2002; Yamamoto and Kitazawa, 2015), suggesting a central mechanism for the perception of a stimulus sequence. Nevertheless, the TO of two visual stimuli, with a gap of less than 20 msec between their onsets, can be processed (subconsciously) and used to optimize task performance (Chassignolle et al., 2021).

Physiological evidence supports the critical ISI of tens of milliseconds as corresponding to the TOT (Joliot et al., 1994; Kujala et al., 2001). Joliot et al. (1994) found a single 40-Hz brain response to a click pair with an ISI<15 msec, but 2 separate 40-Hz waves at longer ISIs. The appearance of the second neuronal oscillation coincided with the perception of both clicks within a pair. This evidence indicates that the first stimulus in a pair initiates a neuronal oscillation with a period of approximately 40 msec and when the second stimulus is processed within the same period of such an oscillation (e.g., an ISI<40 msec), the 2 events are treated as co-temporal and the TO cannot be determined.

TO judgments involve the temporoparietal junction (TPJ) (Eramudugolla et al., 2007: Sinnett et al., 2007; Davis et al., 2009; Woo et al., 2009; Bernasconi et al., 2010a, 2010b; Lewandowska et al., 2010; Wiener et al., 2010; Bernasconi et al., 2011; Adhikari et al., 2013; Takahashi et al., 2013; Binder, 2015; Oron et al., 2015; Lewandowska et al., 2022), a functionally heterogenic region located in the lateral parietal lobe at the junction with the posterior part of the superior temporal gyrus (including portions of the angular gyrus and the supramarginal gyrus) (Bukowski and Lamm, 2017). TO detection has been less precise after damage to either the left (Szelag et al., 2014; Oron et al., 2015) or right TPJ (Eramudugolla et al., 2007; Sinnett et al., 2007).

Magnetoencephalography (MEG) and functional magnetic resonance imaging (fMRI) studies indicate that TO processing involves both TPJs (Davis et al., 2009, Bernasconi et al., 2010a, 2010b, 2011, Lewandowska et al., 2010), but the left one is more activated by accurate TO judgments (Bernasconi et al., 2010a, 2010b, 2011).

The moment-to-moment variability (complexity, temporal dynamics) of resting-state neuronal activity represents the brain's capacity to process information (Garrett et al., 2013; McDonough and Nashiro, 2014; Waschke et al., 2021) and is associated with fluid intelligence (Saxe et al., 2018; Dreszer et al., 2020; Thiele et al., 2023) and creativity (Kaur et al., 2021). It has been argued that neural complexity represents transitions or an exploration of alternative microstates (Honey et al., 2007, 2009; McIntosh et al., 2010; Deco et al., 2011), an optimal noise level in a system that facilitates neuronal firing (Faisal et al., 2008), a balance between functional integration and segregation processes (Tononi et al., 1994) and a degree of randomness in the signal which regulates neuronal synchrony (Ghanbari et al., 2015). The theories of microstates and facilitation of neuronal firing predict a positive relationship between neural complexity and functional connectivity (the temporal coincidence of neurophysiological events) whereas the theory of neuronal synchrony postulates an inverse relationship (i.e., greater neural complexity is associated with weaker functional connectivity) (McDonough and Nashiro, 2014). Electroencephalography (EEG) or MEG techniques with a high temporal resolution appear to be most suitable for capturing rapidly changing resting-state spatiotemporal patterns.

In the current work we used the multivariate MultiScale Entropy (mMSE) algorithm (Ahmed and Mandic, 2011, 2012; Ahmed et al., 2012b, 2012a; Looney et al., 2018), an extension of Sample Entropy (SampEn) measure (Richman and Moorman, 2000; Grundy et al., 2017), to capture repetitive patterns in a resting- state EEG (rsEEG) signal. In contrast to univariate MultiScale Entropy (MSE, Costa et al., 2002), mMSE is suitable for the analysis of multivariate signals, such as EEG, and allows for the examination of their variability across time (scales) and space (electrodes) (Looney et al., 2018). This algorithm was developed to investigate the entropy at fine (short) and coarse (long) timescales (Costa et al., 2002; Ahmed and Mandic, 2011). The interaction between these scales in the brain may represent information exchange in locally and globally distributed neuronal assemblies. Specifically, fine scales are linked with short-distance connections in the brain whereas coarse scales represent long-range interactions between regions/networks (Vakorin, 2011; McIntosh et al., 2014; Wang et al., 2018).

In the present study, we hypothesized that the visual TOT, as an index of temporal resolution, would be associated with the temporal dynamics of rsEEG activity. This relationship could be either negative or positive. As already stated, accurate TO identification is linked to efficient information processing and fluid intelligence (e.g., Szymaszek et al., 2009; Ulbrich et al., 2009; Pahud et al., 2018). Well-functioning biological systems are thought to produce complex signals (with a broad

range of dynamic variability), which enable adaptation to a constantly changing environment (Costa et al., 2002). In support of this view, brain entropy has been associated with intelligence (Saxe et al., 2018; Dreszer et al., 2020) and reduced neural complexity levels have been found in a variety of central nervous system (CNS) disorders including Alzheimer's disease (Mizuno et al., 2010; Li et al., 2018), autism (Catarino et al., 2011), depression (Zhang et al., 2015) and ADHD (Sokunbi et al., 2013; Gu et al., 2022). In light of this evidence, we may expect low TOT values to be associated with high rsEEG entropy levels.

However, it is worth noting that the relationships between resting-state neural complexity and intelligence vary across different regions and timescales (Dreszer et al., 2020; Thiele et al., 2023) and CNS disorders could be characterized by increased brain complexity compared to healthy controls (Bosl et al., 2017; Ho et al., 2017; Zhang et al., 2021). Therefore, an inverse relationship between TOT and rsEEG entropy is also possible. According to Ghanbari et al. (2015), more regular and predictable signals are low in complexity, which increases information processing across distributed regions. Consistent with this theory, low neural complexity could be beneficial for TO perception.

We also hypothesized that TO identification would involve the neuronal mechanism ensuring the time frames for general cognitive functioning and behavior (Pöppel et al., 2011) and, as so, would be associated with global information processing in the resting brain (Bullmore and Sporns, 2009; Power et al., 2011). Neural complexity at coarse timescales reflects long-range interactions between regions/networks (Courtiol et al., 2016) and refers to a relatively stable brain state and the transitions between these states. Considering the above-mentioned theories linking neural complexity to the range of microstates (Honey at al., 2007; McIntosh et al., 2010) and regulation of neural synchrony (Ghanbari et al., 2015) it is difficult to predict whether high or low degrees of coarse rsEEG complexity would facilitate information processing, and, therefore, be associated with low TOT values.

TO processing involves bilateral activation of the TPJ (Davis et al., 2009; Bernasconi et al., 2010b), and, the left TPJ's activity is particularly related to the accuracy of TO judgments (Bernasconi et al., 2010a; Lewandowska et al., 2022). Therefore, we assumed that the visual TOT would be associated with the rsEEG entropy measures obtained from the electrodes placed over the left temporo-parieto-occipital cortex. Considering the involvement of attention/working memory in TO judgments and the possibility of using a holistic strategy in this task (i.e., integrating 2 single stimuli into one percept, McFarland et al., 1998, Szelag et al., 2018), TOT may be also related to rsEEG complexity calculated for channel sets placed in other locations on the scalp such as the central or frontal areas.

METHODS

Subjects

Seventy one high school students, recruited in the area of Toruń, Poland (37 women and 34 men; mean age=17.48±0.95 years, age range: 16-19 years) comprised the final study sample after excluding 6 subjects due to either excessive movement during the EEG data acquisition or abnormally high (>150 msec) TOT values. All participants attended school regularly, were in good health, reported no history of neurological/psychiatric disorders and declared themselves not to be taking any medicines affecting the CNS. All the participants were all right-handed and had a normal or corrected-to-normal vision.

The study was approved by the Bioethics Committee of the Nicolaus Copernicus University in Toruń, operating at Collegium Medicum in Bydgoszcz, Poland (permission no. KB 196/2016) and was conducted in accordance with the Declaration of Helsinki. All subjects, prior to participation in the study, gave written informed consent to take part. Minors provided additional consents from their parents/caregivers. Moreover, all the participants received monetary remuneration for their time and effort.

Each subject underwent a psychophysical TOT assessment and took part in an rsEEG study. These procedures were administered within two separate sessions in one day and their order was counterbalanced across the participants.

Psychophysical visual TO judgment task

TOT evaluation was conducted individually in an acoustically shielded chamber. The stimuli were pairs of 40-msec light flashes emitted by diodes mounted to the wall in front of the subjects in 2 different locations on a horizontal line. The diodes were placed 41 cm and 40 cm away from the fixation point (a diode) on its left and right sides, respectively. A subject was seated at a table that was 75 cm high on a chair that was 47 cm high, at a distance of 161 cm from the fixation point and was asked to keep the head on a chin rest during the entire procedure. The viewing angle of the stimulation was 29.27°. The procedure was controlled using a Raspberry Pi 3 Model B SBC (Bulk) equipped

with an Arduino Genuine Zero microcontroller. The stimuli were generated by an LED Maxim Integrated MAX16822BEVKIT+ controller and presented via a white LED CREE diodes with a maximum luminance of 350 lm.

Two response pads were connected to the computer using optical fibers to ensure the least possible delay in signal transmission. A subject held one response pad in each hand and was requested to press, using the thumb, as quickly as possible, the right or the left key, depending on which side the first diode in the pair appeared.

The task consisted of 100 consecutive stimulus pairs, separated by an inter-trial interval of 3 sec. The main task was preceded by 10 practice trials. TOT was determined individually in each subject. As with previous studies (Szymaszek et al., 2009; Ulbrich et al., 2009; Jablonska et al., 2020), TOT was defined as the ISI for which a 75% correctness level was achieved. The TOT values were obtained based on *post hoc* estimation of the psychometric curve from all the available trials made during the task. The data were fitted using the Psignifit 4 toolbox implemented in Matlab (Schütt et al., 2016). The psychometric curves, determined individually for each subject, are shown in Fig. S1 in the Supplementary Materials.

EEG data acquisition and pre-processing

For each subject, a 10 min rsEEG signal with eyes closed was obtained from 64 electrodes placed on the scalp according to the 10-10 system using the Brain Products BrainAmp EEG system. A reference electrode was positioned at FCz and the sampling rate was set at 1000 Hz. The impedance was kept below 10 kΩ during the entire data registration process.

Subjects were seated in an upright relaxed position. Prior to EEG data recording, they were asked to refrain from any movements and "not to think about anything specific and let the thoughts run freely". The EEG signal was pre-processed using EEGLAB ver.2020 (Delorme and Makeig, 2004) for Matlab (Mathworks Inc.). The signal was filtered (bandpass: 1-40 Hz) and down-sampled to 256 Hz. High amplitude artifacts were removed from the signal using the trimOutlier function, and the remaining data was re-referenced to the average (common) reference. Next, the EEG data was decomposed using the Infomax Independent Component Analysis (ICA) algorithm (Bell and Sejnowski, 1995). The components classified as artifacts by the two toolboxes: Mara (Winkler et al., 2011, 2014) and Adjust (Mognon et al., 2011) were rejected (M=40.74±7.66 across subjects). The signal was then visually inspected and any remaining artifacts were removed manually.

A maximum number of 40-sec uncut fragments of EEG signal was extracted from each individual dataset. In each participant, the first fragment, obtained after approximately 2 min of data acquisition, was analyzed to provide signal samples that represent the moments of a relatively similar state of mind in the whole study group. It seems reasonable to believe that after 2 min of participating in the rsEEG study, the subjects would manage to settle in a resting state, be calm, relaxed, but not yet bored, tired, or drowsy.

MMSE analysis

The rsEEG signal was analyzed using the mMSE algorithm (Ahmed and Mandic, 2011; Ahmed et al., 2012a), which estimates sample entropy at various timescales and electrode sets. mMSE is the extension of MSE based on the SampEn algorithm (Richman and Moorman, 2000) that uses a coarse-graining procedure (Costa et al., 2002, 2005) to evaluate biological signals' variability across timescales. SampEn provides reproducible patterns of signal over time. The temporal graining procedure in the frequency domain acts as a low-pass filter and mitigates linear effects between successive samples in a signal (Costa et al., 2002). In contrast to the univariate MSE that only allows the determination of temporal complexity profiles, mMSE measures signal complexity in the spatiotemporal domain (refer to Dreszer et al., 2020, for a detailed explanation of this algorithm).

We obtained the mMSE vectors in each participant for the following channel sets (Fig. 1): central (midline, CE: Fz, Cz, Pz and Oz), left anterior (LA: Fp1, F3, Fc5 and F7), right anterior (RA: Fp2, F4, Fc6 and F8), left middle (LM: T7, C3, Cp1 and Cp3), right middle (RM: T8, C4, Cp2 and Cp4), left posterior (LP: P3, P7, PO3 and O1) and right posterior (RP: P4, P8, PO4 and O2). In all of these cases, the mMSE vectors were stable and characterized by a skewed inverted-U shape across time scales (Fig. 2), which had also been observed in previous studies (Costa et al., 2002, 2005; McDonough and Nashiro, 2014; McIntosh et al., 2014; Ahammed and Ahmed, 2020; Dreszer et al., 2020; Omidvarnia et al., 2021; Gu et al., 2022). Such an mMSE vector shape is considered as representing more random signals at fine scales and a highly stable activity at coarse scales (Costa et al., 2005; McIntosh, 2018).

Three features of the mMSE vectors were analyzed: the area under curve (AUC), the MaxSlope and the AvgEnt. AUC is obtained from a trapezoidal approximation of the area delimited by the mMSE vector and is considered to reflect the total EEG complexity. MaxSlope is the maximum pairwise difference between the

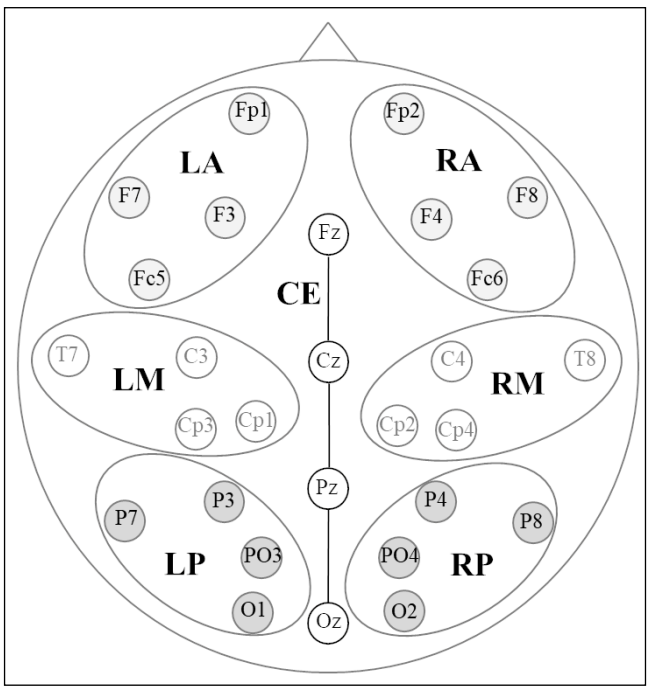

Fig. 1. Channel sets locations. CE – central, LA – left anterior, LM – left middle, LP – left posterior, RA – right anterior, RM – right middle, RP – right posterior.

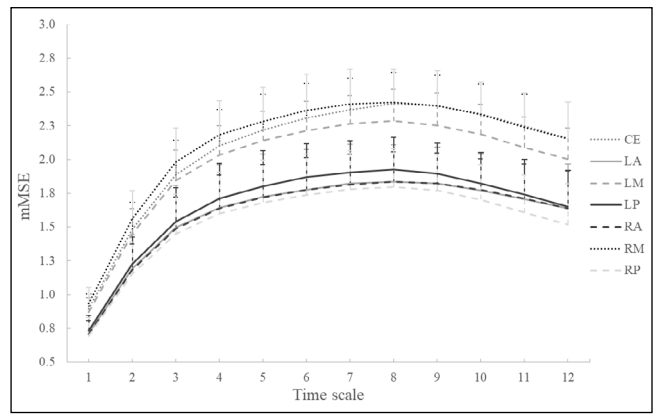

Fig. 2. The skewed inverted-U shapes of the mMSE vectors for each channel set in the whole sample. The x-axis represents timescales and the y-axis shows the average of the mMSE values across the subjects. Error bars represent standard deviations. The mMSE vectors were calculated using the following parameters for all electrode sets: m=2, r=0.15, p=4, ε=12, where m is the embedding coefficient, r is the similarity threshold, p is the number of electrodes in a given electrode set, and ε is the timescale. The time delay τk was set to 1 for k=1,2,...,p. CE – central, LA – left anterior, LM – left middle, LP – left posterior, RA – right anterior, RM – right middle, RP – right posterior.

first four timescales of the mMSE vector divided by the indices' difference. MaxSlope represents the maximum complexity change of the EEG signal at high-frequency fine scales. AvgEnt is defined as the average value of the last 4 elements (9:12 temporal scales) of the mMSE vector, and it is regarded as reflecting the baseline entropy of the EEG signal at low-frequency coarse scales. The scripts used to determine all these features can be found at https://github.com/IS- UMK/complexity/tree/master/MMSE_features.

Statistical analysis

Considering previous studies indicate that men outperform women in TO judgment tasks (Lotze et al., 1999; Wittmann and Szelag, 2003; Fink et al., 2005; Szymaszek et al., 2006; Ulbrich et al., 2009) and young adults are more accurate than children and adolescents in TO identification (Berwanger and Wittmann, 2004; Edmonds et al., 2008), we first checked whether gender and age of our subjects affect TOT. Distribution of the TOT values and age in our study did not show significant deviations from normality (the Shapiro-Wilk test); therefore, we used the independent samples t-test to compare the TOT between men and women and the Pearson's correlations to examine the relationship between TOT and age.

We are also aware of gender differences in resting-state neural complexity (Luders et al., 2004; Pravitha et al., 2005; Fernández et al., 2012; Ahmadi et al., 2013; Kumral et al., 2020; Wang, 2021). Therefore, in the current study, we tested whether men and women are different in terms of AUC, MaxSlope and AvgEnt values.

Since the distributions of these entropy parameters did not show significant deviations from normality, ANOVA with "Area" (CE, LA, RA, LM, RM, LP and RP) as a repeated measure and "Gender," as a between-subject factor, was performed separately for each mMSE feature. The results were adjusted using the Greenhouse-Geisser Correction.

Age-related differences in neural complexity at rest (McIntosh et al., 2008; Miskovic et al., 2016; Jia et al., 2023) led us to verify whether in the current study age affects the features of mMSE vectors, calculated for particular channel sets. Finally, the Pearson correlations of the TOT with the AUC, AvgEnt and MaxSlope were calculated separately for each electrode set (area). The P values were adjusted for multiple testing through the use of false discovery rate (FDR, Benjamini and Hochberg, 1995).

All statistical analyses were performed using the R package (R Core Team 2020).

RESULTS

Behavioral results

The mean TOT was 41.35±13.66 msec and TOT values were between 15.88 and 77.66 msec. The skewness and kurtosis of TOT was 0.589 and -0.017, respectively. No significant ($t69$=0.926, P=0.358) differences in the TOT were found between men (mean TOT=39.79 msec, SD=14.74 msec, the TOT range: 15.88-77.66 msec) and women (mean TOT=42.8 msec, SD=12.63 msec, the TOT range: 20.8-71.19 msec). TOT not significantly correlated with age (r=-0.153, P=0.202).

MMSE results

Descriptive statistics for the mMSE features in particular regions are shown in Table 1. The main effect of "Area" was significant in the case of AUC ($F4.293, 296.244$=236.228, P<0.001, η^2p=0.774), MaxSlope ($F4.597,317.210$=196.087, P<0.001, η^2p=0.740) and AvgEnt ($F4.323,298.271$=242.774, P<0.001, η^2p=0.779). The results of *post-hoc* comparisons of the AUC, MaxSlope and AvgEnt between particular channel sets are shown in Tab. S1 in the Supplementary Materials.

Considering the AUC, neither a main effect of "Gender" ($F1,69$=0.65, P=0.423, η^2p=0.009) nor an "Area" × "Gender" interaction ($F4.293,296.244$=0.649, P=0.639,

Table 1. Descriptive statistics (mean, standard deviation, skewness and kurtosis) for three features (AUC, MaxSlope and AvgEnt), derived from the multivariate MultiScale Entropy (mMSE) vectors, calculated for the central (CE), left anterior (LA), left middle (LM), left posterior (LP), right anterior (RA), right middle (RM) and right posterior (RP) channel sets.

Variable		M	SD	Skewness	Kurtosis
AUC	CE	23.29	2.27	-0.450	0.530
	LA	17.96	2.99	-0.325	0.014
	LM	22.20	2.02	-0.276	5.414
	LP	18.63	2.41	-0.419	-0.025
	RA	17.94	2.33	-0.074	0.826
	RM	23.72	2.35	-1.232	3.195
	RP	17.38	2.89	-0.237	0.642
MaxSlope	CE	0.40	0.06	-0.098	-0.589
	LA	0.31	0.07	-0.383	-0.212
	LM	0.39	0.04	-1.134	2.561
	LP	0.33	0.05	-0.392	-0.120
	RA	0.31	0.05	-0.243	0.519
	RM	0.42	0.05	-0.810	1.041
	RP	0.30	0.06	-0.260	-0.023
AvgEnt	CE	2.29	0.22	-0.256	0.512
	LA	1.73	0.28	-0.335	0.295
	LM	2.13	0.21	-0.660	3.292
	LP	1.78	0.24	-0.438	-0.381
	RA	1.74	0.24	0.159	1.154
	RM	2.28	0.24	-0.713	2.164
	RP	1.65	0.27	-0.059	0.586

η^2p=0.009) was significant. For the MaxSlope, a main effect of "Gender" (*F1,69*=0.766, *P*=0.385, η^2p=0.011) and an "Area" × "Gender" interaction (*F4.597,317.210*=0.596, *P*=0.689, η^2p=0.009) were both not meaningful, as were the effects for the AvgEnt (the main effect of "Gender": *F1,69*=0.276, *P*=0.601, η^2p=0.004 and "Area" × "Gender" interaction: *F4.323,298.271*=0.557, *P*=0.708, η^2p=0.008). None of these features of mMSE vectors significantly correlated with age (Tab. S2 in the Supplementary Materials).

Because we did not find any meaningful gender-related differences in TOT, AUC, MaxSlope and AvgEnt values, a correlation analysis between the TOT and the features of mMSE vectors was performed on the whole sample (n=71). There were no significant correlations of age with TOT, AUC, MaxSlope and AvgEnt, therefore, the relationship between the TOT and the rsEEG entropy measures was tested without controlling for the age factor.

The greater were the AUC values in the CE, LP, RP and RM regions as well as the greater was the AvgEnt values in the CE, LP and RP areas, the higher was the visual TOT. The most robust associations (*r*=0.366, *P*=0.018, and *r*=0.397, *P*=0.013 for AUC and AvgEnt, respectively, with FDR correction for multiple comparisons, *P*<0.05) were found for the midline channel set (Fz, Cz, Pz, and Oz). There were no significant correlations between the TOT and the MaxSlope parameters. Table 2 contains the outcomes of Pearson's correlation analysis between the TOT and the AUC, MaxSlope and AvgEnt features of mMSE vectors. The scatter plots illustrating the relationships between the TOT and the mMSE parameters are shown in Figs 3-5.

Table 2. The results of correlation analysis between the visual temporal order threshold (TOT) and the three features (AUC, MaxSlope and AvgEnt), derived from the multivariate MultiScale Entropy (mMSE) vectors, calculated for the central (CE), left anterior (LA), left middle (LM), left posterior (LP), right anterior (RA), right middle (RM) and right posterior (RP) channel sets.

		r	*P* value (uncorrected)	*P* value (FDR corrected)
AUC	CE	0.366	0.002**	0.018*
	LA	0.098	0.415	0.436
	LM	0.233	0.05*	0.081
	LP	0.317	0.007**	0.034*
	RA	0.226	0.058	0.086
	RM	0.304	0.01**	0.035*
	RP	0.294	0.013*	0.039*
MaxSlope	CE	0.244	0.04*	0.077
	LA	0.08	0.509	0.509
	LM	0.223	0.062	0.086
	LP	0.262	0.027*	0.057
	RA	0.192	0.108	0.133
	RM	0.269	0.023*	0.054
	RP	0.234	0.049*	0.081
AvgEnt	CE	0.397	0.001**	0.013*
	LA	0.106	0.38	0.42
	LM	0.143	0.235	0.274
	LP	0.313	0.008**	0.034*
	RA	0.193	0.107	0.133
	RM	0.271	0.022*	0.054
	RP	0.312	0.008**	0.034*

The "**" symbol represents P<0.01, whereas the "*" symbol indicates P<0.05. The *r* represents the Pearson's correlation coefficients and FDR – False Discovery Rate.

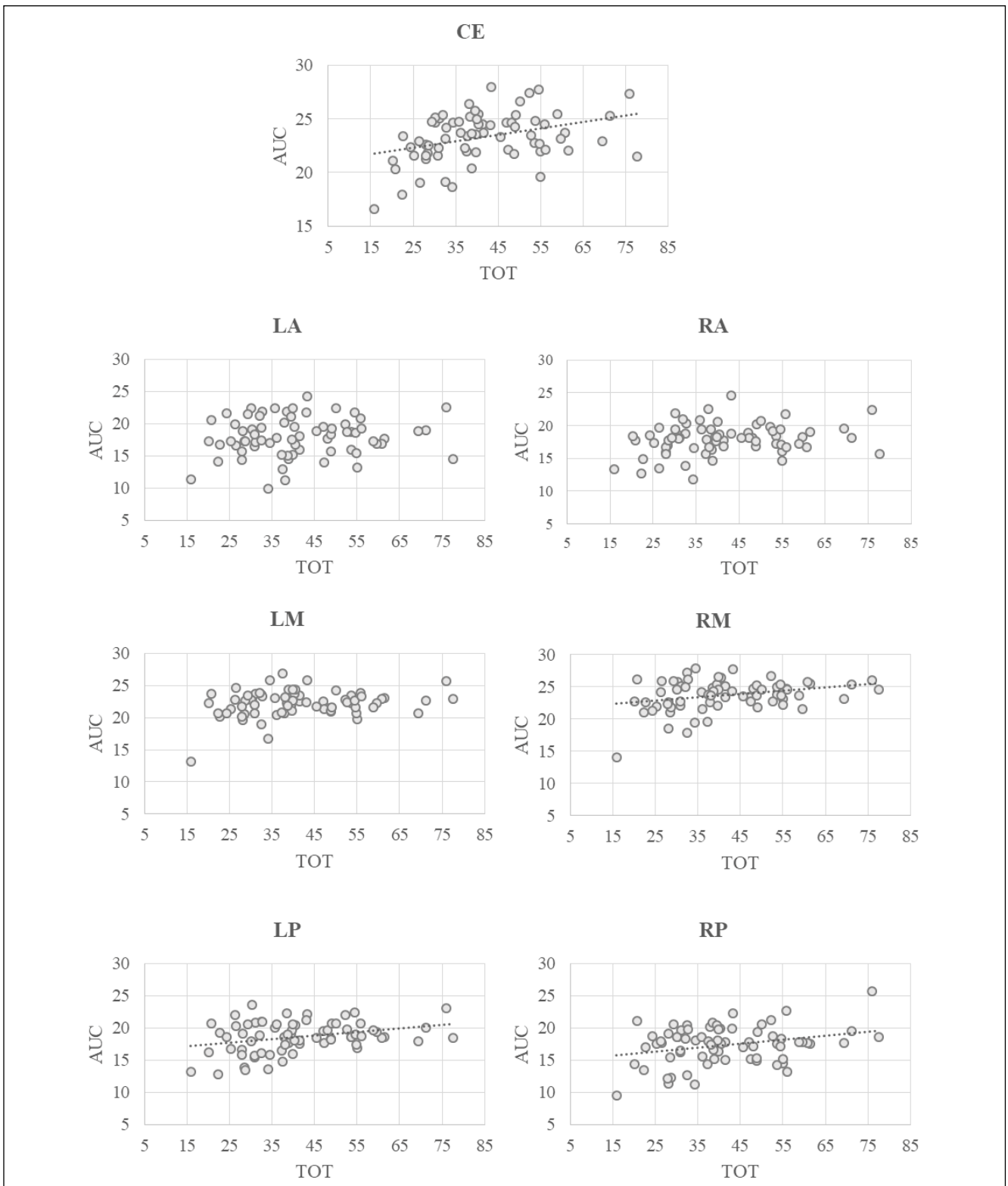

Fig. 3. The scatterplots demonstrating the Pearson's correlations between the visual temporal order threshold (TOT) and the AUC feature of multivariate MultiScale Entropy (mMSE) vectors determined based on resting-state EEG signal separately for the electrode sets corresponding to the following seven scalp regions: central (midline, CE), left anterior (LA), left middle (LM), left posterior (LP), right anterior (RA), right middle (RM) and right posterior (RP). X axis represents the TOTs and Y represents the AUC feature. In the case of significant (P<0.05) associations between the TOT and the AUC values, the trend lines are shown in the scatterplots.

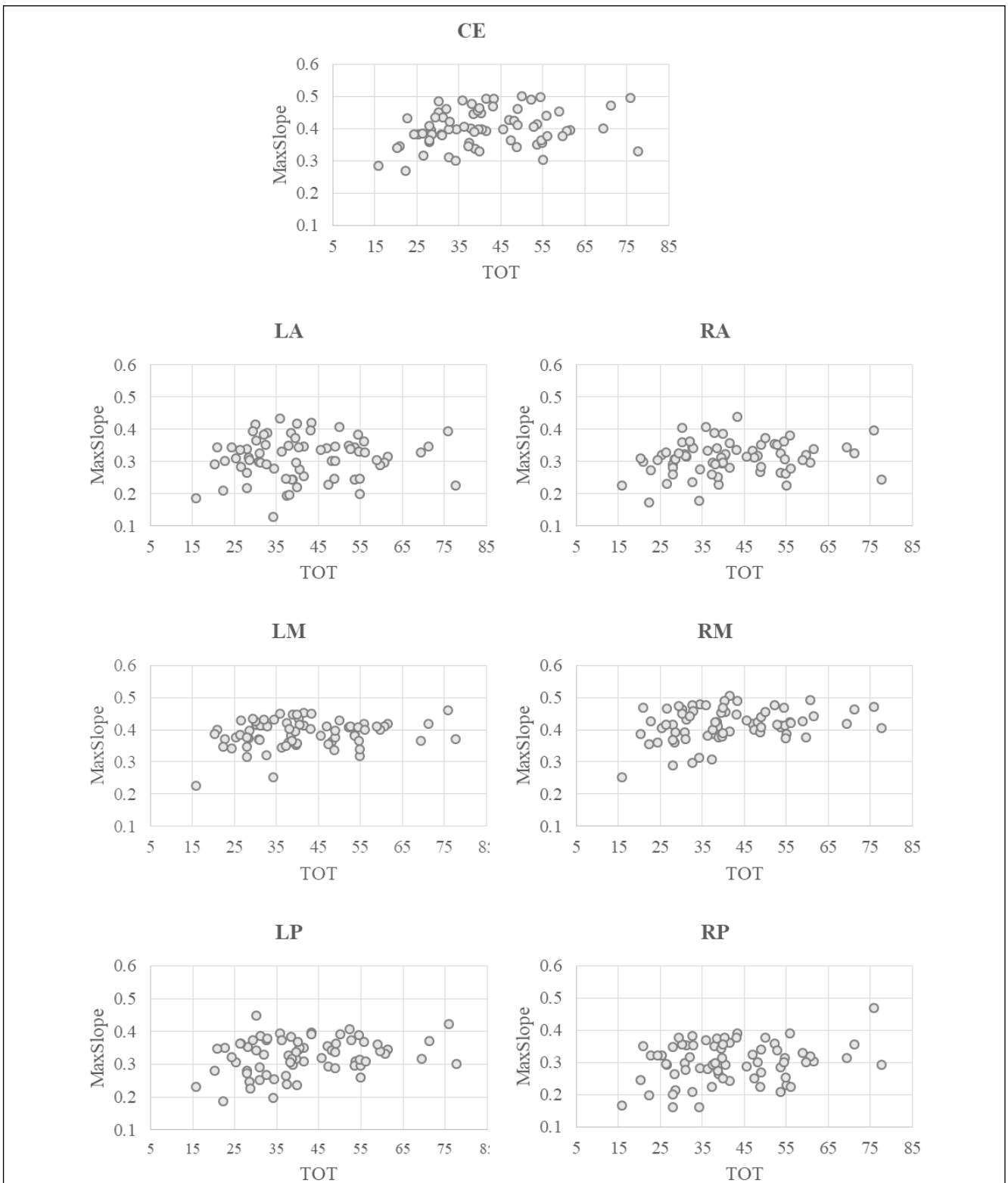

Fig. 4. The scatterplots demonstrating the Pearson's correlations between the visual temporal order threshold (TOT) and the MaxSlope feature of multivariate MultiScale Entropy (mMSE) vectors determined based on resting-state EEG signal separately for the electrode sets corresponding to the following seven scalp regions: central (midline, CE), left anterior (LA), left middle (LM), left posterior (LP), right anterior (RA), right middle (RM) and right posterior (RP). X axis represents the TOTs and Y represents the AUC feature. In the case of significant (P<0.05) associations between the TOT and the AUC values, the trend lines are shown in the scatterplots.

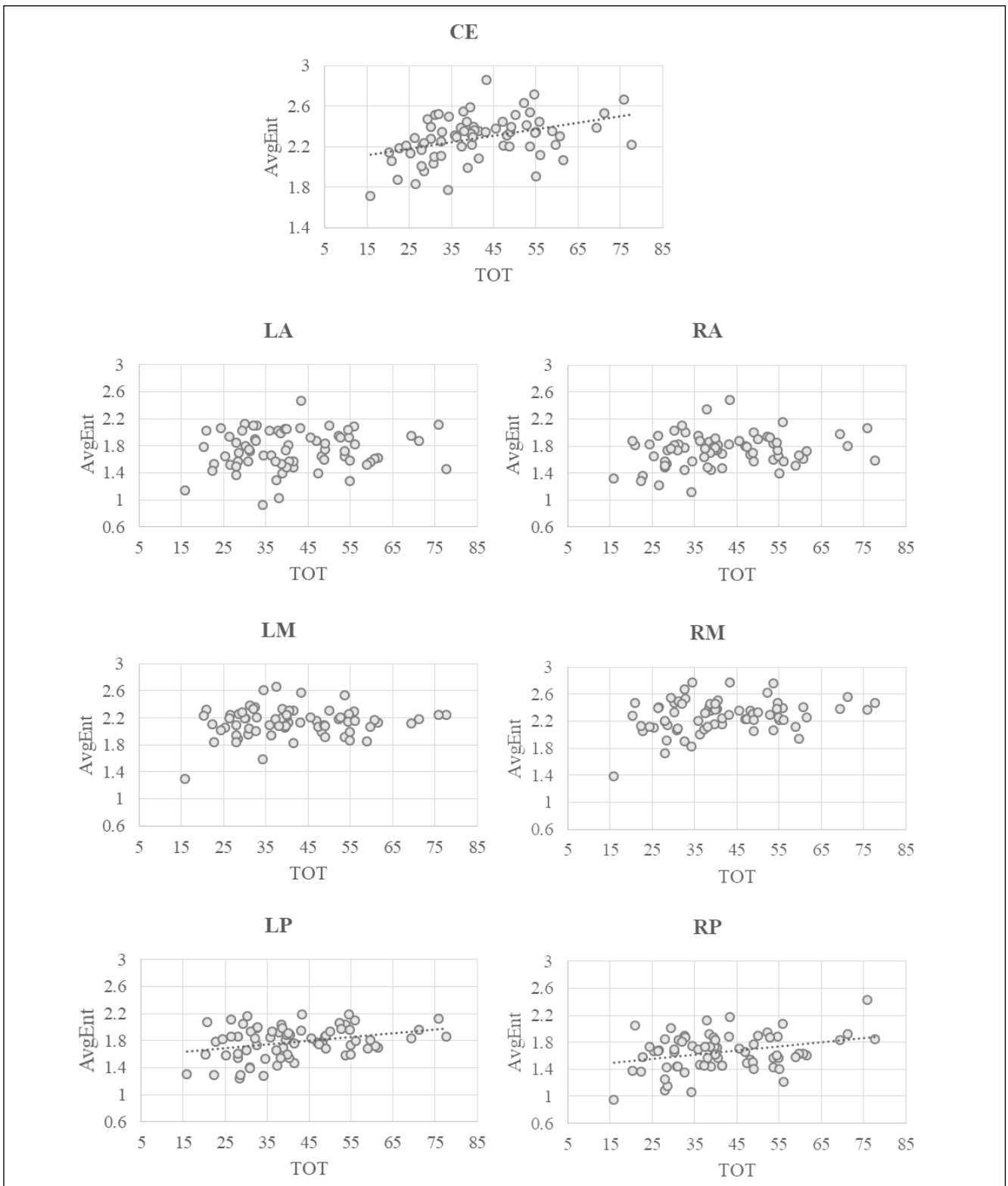

Fig. 5. The scatterplots demonstrating the Pearson's correlations between the visual temporal order threshold (TOT) and the AvgEnt feature of multivariate MultiScale Entropy (mMSE) vectors determined based on resting-state EEG signal separately for the electrode sets corresponding to the following seven scalp regions: central (midline, CE), left anterior (LA), left middle (LM), left posterior (LP), right anterior (RA), right middle (RM) and right posterior (RP). X axis represents the TOTs and Y represents the AUC feature. In the case of significant (P<0.05) associations between the TOT and the AUC values, the trend lines are shown in the scatterplots.

DISCUSSION

To the best of our knowledge this is the first study demonstrating the relationship between visual TOT, and rsEEG complexity as assessed using the mMSE algorithm. Although this method has been rarely used to quantify neural complexity (Azami et al., 2017, 2019; Ahammed and Ahmed, 2020; Dreszer et al., 2020), it appears to be a promising tool to investigate individual differences in cognition. MMSE is suited for analyzing the signals registered from many channels and allows entropy to be determined at fine and coarse timescales (Ahmed and Mandic, 2011, 2012). In light of the proposed theories elucidating functional significance of neural complexity (McIntosh et al., 2014), including these scales to data analysis might provide information about short- and long-range interactions between neuronal assemblies.

The less complex the pattern of rsEEG activity, the lower the visual TOT In this study it was reasonable to assume high rsEEG entropy to be associated with low TOT values. Firstly, because increased neural complexity may indicate greater transition/exploration between different states of networks, thereby, greater functional connectivity/information processing (Honey et al., 2007, 2009; McIntosh et al., 2010; McDonough and Nashiro, 2014; Wang et al., 2018); secondly, fluid intelligence, defined as an ability to solve novel problems and adapt to environmental demands (Cattell, 1963), is positively related to resting-state brain complexity (Saxe et al., 2018; Dreszer et al., 2020) and negatively to TOT (Rammsayer and Brandler, 2007; Ulbrich et al., 2009). However, contradictory to above assumption, we found low visual TOT values linked with reduced total and coarse rsEEG entropy levels obtained from the central, posterior and the right middle electrode sets. Therefore, decreased rsEEG complexity of the regions/networks contributing to these channels, might be beneficial for TO judgments. Considering greater neural complexity to be associated with greater functional connectivity (McIntosh et al., 2010), the current results are consistent with our previous fMRI study demonstrating a positive relationship of the left TPJ's functional couplings at rest with visual TOT (Lewandowska et al., 2022). Furthermore, other authors found efficient perceptual/procedural learning to be associated with decreased number of resting-state interactions in the sensorimotor network (Vahdat et al., 2011, 2014; Mary et al., 2017; Van Dyck et al., 2021).

An alternative explanation of the positive relationship between rsEEG entropy and TOT comes from the theory suggesting that low degrees of temporal variability in a system (predictable and regular signals) ensure an environment that facilitates the probability of synchrony between areas (Ghanbari et al., 2015). RsEEG signal with a low entropy level (increased information exchanged across regions at rest), associated with low TOT values may suggest better regulation of the CNS, thus, the system exhibits optimal functioning when TO is assessed correctly at shorter ISIs.

In line with our predictions, the visual TOT was positively associated with the AvgEnt reflecting entropy at coarse scales. Considering the theory that links coarse neural complexity with long-distance connections (Vakorin, 2011; McIntosh et al., 2014; Wang et al., 2018), a positive relationship between temporal variability of rsEEG signal and visual TOT might indicate that decreased global information processing at rest provides a favorable environment for TO perception. Therefore, TOT could be considered an index of a mechanism providing the time frames for cognition and behavior which are underpinned by large-scale functional networks. It is also worth noting that low complexity at coarse scales is associated with great white matter integrity (McDonough and Siegel, 2018). Therefore, our results might suggest that maintaining a high level of structural interconnections across distributed neuronal populations promotes the TO identification.

We did not find any significant correlations between visual TOTs and the measure of fine complexity which is thought to represent local information processing and within-hemispheric functional connections (McIntosh et al., 2014). Thus, our outcomes may indicate that the interconnectivity among local neural populations is unrelated to the accuracy of TO judgments.

In the section below, we discussed the relationship between rsEEG entropy and TOT, referring to the processes that might be involved in the TO judgments.

RsEEG complexity is positively associated with visual TOT, serving as an index of cognitive processing, temporal resolution or feature-specific discrimination.

The identification of TO of two rapidly incoming events definitely requires cognitive effort, attention and working memory (Fink et al., 2006b; Szymaszek et al., 2009; Ulbrich et al., 2009). Since the subjects are able to focus attention more efficiently on the stimuli presented in rapid succession, they can also report the TO of the light flashes at shorter ISIs. Taking into account that lower resting-state brain entropy is associated with higher task-related information processing (Lin et al., 2022), reduced rsEEG complexity levels linked with lower TOT values may reflect higher activations of the regions subserving attention and cognitive effort during the TO judgment task. In support of this notion, we found the most robust relationships of the TOT with the total and coarse rsEEG entropy measures for the midline electrodes which receive contributions from the areas/networks involved in atten-

tion and working memory (Polich, 2007; Giacometti et al., 2014; Sabeti et al., 2015; Łaszewska et al., 2018). Furthermore, in our study, the TOT was significantly associated with the rsEEG entropy, determined for the channels placed over the posterior and right middle regions that are likely to be engaged in attentional processing (Corbetta and Shulman, 2002; Behrmann et al., 2004). However, since these electrodes do not receive only temporal or parietal contributions, the above conclusions should be taken with caution.

Consistent with previous studies (Hirsh and Sherrick, 1961; Lotze et al., 1999; Wittmann, 1999; Kanabus et al., 2002; Fink et al., 2006b; Ulbrich et al., 2009; Chassignolle et al., 2021) we found an average visual TOT of approximately 40 msec and some individual temporal threshold values of ≤20 msec. According to the hypothesis of a central timing mechanism (Joliot et al., 1994; Pöppel, 1994, 1997) the TO of two sensory events can be determined when they are separated by more than 30 msec. For lower TOT values, the feature-specific discrimination mechanisms allowing for the integration of two successive stimuli into one percept, are likely to be involved. In other words, the ability to judge TO depends on whether a task requires actual identification of the individual events of the sequence or whether the task could be performed by discrimination of a global pattern. In our study, two light flashes appearing rapidly at different positions might have produced the impression of apparent motion, which activates neurons in motion-sensitive areas (Craig and Busey, 2003; Seiffert, 2003). In that case, a TO judgment task becomes "atemporal" since the TO of two stimuli is extracted from the motion percept. Similar feature-specific discrimination mechanisms have been described in the context of TO perception of tactile or auditory events. Specifically, judging which of two sites on a hand was stimulated first may rely on the direction of motion across fingers (Craig and Busey, 2003) whereas the before-after relation between two tones differing in pitch can be determined by integrating them into a single sound of rising or falling frequency (Micheyl et al., 2007; Szelag et al., 2018). Therefore, TO judgment tasks should be considered not only as involving a central timing mechanism but also different perceptual strategies.

When two distinct sensory events could be perceived (ISI≥30 msec), the TOT is more likely to be considered an index of temporal information processing, i.e., first the identification of incoming stimuli within a sequence and, then, the TO perception. Therefore, the positive relationship between TOT and rsEEG entropy may indicate that the more complex the spatiotemporal patterns at rest, the higher contribution of "pure" timing to the TO judgment task. In other words, high rsEEG complexity levels may reflect a greater capacity, preparation or readiness of the brain to identify the TO relying on a timing mechanism. In support of this view, we found higher TOT values to be associated with greater complexity of rsEEG signal from the right and left posterior electrode sets which cover the TPJ, considered a neural substrate for TO perception (Davis et al., 2009; Bernasconi et al., 2010b). However, the channels located in the these areas not necessarily receive signals from the TPJ, and definitely not only from this region.

Conversely, stimulus-specific perceptual mechanisms could be engaged to a great extent in the case of an ISI<30 msec. "Sensing" the motion while judging the TO requires an adaptation to process non- temporal features of visual stimuli which activates the motion-sensitive regions. In line with this conclusion, we found TOT correlated positively with rsEEG entropy for the channel sets placed over the temporal, parietal and occipital cortices which are involved in motion perception (Seiffert, 2003; Noguchi et al., 2005). Therefore, lower rsEEG complexity in the right middle and both posterior channel sets associated with lower visual TOTs in our study, may indicate using a global strategy to cope with brief ISIs. In other words, reduced rsEEG entropy levels may facilitate adaptation of the (brain) system to process non-temporal properties of visual stimuli in TO judgment tasks.

The study limitations and future directions

The current study has several limitations which should be kept in mind while interpreting the outcomes. The mMSE algorithm used here to determine rsEEG complexity, has some constraints that were discussed in details in our previous work (Dreszer et al., 2020, Section 4.3.). A sample size could be larger, especially since individual differences were examined. We calculated only correlations between the TOT and the rsEEG signal entropy, which does not imply any causal relationship between these variables. Linking brain signal complexity at fine or coarse scales to local or global information processing, respectively, is questionable (Kosciessa et al., 2020; Omidvarnia et al., 2021).

Future studies should examine whether rsEEG signal complexity is also related to TOTs measured for other sensory modalities (auditory and tactile). Since the mMSE algorithm is not commonly used to investigate EEG activity dynamics, the reliability of this method should be checked. It would be also advisable to consider brain anatomy while interpreting neural complexity outcomes especially information about white matter

microstructure (McDonough and Siegel, 2018). A source analysis of EEG activity would provide brain locations of the signals for which the mMSE features have been determined.

CONCLUSIONS

The current study is the first to demonstrate that perceiving the TO of two events, presented in rapid succession, is associated with the temporal dynamics of spontaneous EEG activity. The lower total and coarse entropy levels of rsEEG signal obtained from the midline, right middle, right and left posterior electrode sets, the lower the visual TOT, assessed in the psychophysical experiment. This relationship between rsEEG complexity and TOT might suggest reduced temporal variability of spontaneous brain signal to facilitate TO identification. Considering the coarse timescales as reflecting long-distance interactions across distributed neural assemblies, our findings might support the role of large-scale connections in the TO perception. Further studies are needed to clarify these issues.

ACKNOWLEDGMENTS

The study was founded by the National Science Centre grant no. 2015/18/E/HS6/00399. We would like to thank Joanna Gorgol and Jan Nikadon for help with data collection. We are also very grateful to our participants for their time and effort.

REFERENCES

Adhikari BM, Goshorn ES, Lamichhane B, Dhamala M (2013) Temporal-order judgment of audiovisual events involves network activity between parietal and prefrontal cortices. Brain Connect 3: 536–545.

Ahammed K, Ahmed MU (2020) Quantification of mental stress using complexity analysis of EEG signals. Biomed Eng Appl Basis Commun 32: 2050011.

Ahmadi K, Ahmadlou M, Rezazade M, Azad-Marzabadi E, Sajedi F (2013) Brain activity of women is more fractal than men. Neurosci Lett 535: 7–11.

Ahmed MU, Mandic DP (2011) Multivariate multiscale entropy: A tool for complexity analysis of multichannel data. Physical Review E 84: 061918.

Ahmed MU, Mandic DP (2012) Multivariate multiscale entropy analysis. IEEE Signal Process Lett 19: 91–94.

Ahmed MU, Rehman N, Looney D, Rutkowski TM, Kidmose P, Mandic DP (2012a) Multivariate entropy analysis with data-driven scales. IEEE International Conference on Acoustics, Speech and Signal Processing, Publisher: IEEE, 3901–3904.

Ahmed MU, Rehman N, Looney D, Rutkowski TM, Mandic DP (2012b) Dynamical complexity of human responses: a multivariate data-adaptive framework. Bull Pol Acad Sci Tech Sci 60(3).

Azami H, Abásolo D, Simons S, Escudero J (2017) Univariate and multivariate generalized multiscale entropy to characterise EEG signals in Alzheimer's disease. Entropy 19: 31.

Azami H, Fernández A, Escudero J (2019) Multivariate multiscale dispersion entropy of biomedical times series. Entropy 21: 913.

Behrmann M, Geng JJ, Shomstein S (2004) Parietal cortex and attention. Curr Opin Neurobiol 14: 212–217.

Bernasconi F, Grivel J, Murray MM, Spierer L (2010a) Plastic brain mechanisms for attaining auditory temporal order judgment proficiency. NeuroImage 50: 1271–1279.

Bernasconi F, Grivel J, Murray MM, Spierer L (2010b) Interhemispheric coupling between the posterior sylvian regions impacts successful auditory temporal order judgment. Neuropsychologia 48: 2579–2585.

Bernasconi F, Manuel AL, Murray MM, Spierer L (2011) Pre-stimulus beta oscillations within left posterior sylvian regions impact auditory temporal order judgment accuracy. Int J Psychophysiol 79: 244–248.

Berwanger D, Wittmann M (2004) Measurement of temporal-order judgment in children. Acta Neurobiol Exp 64: 387–394.

Binder M (2015) Neural correlates of audiovisual temporal processing – Comparison of temporal order and simultaneity judgments. Neuroscience 300: 432–447.

Bosl WJ, Loddenkemper T, Nelson CA (2017) Nonlinear EEG biomarker profiles for autism and absence epilepsy. Neuropsychiatr Electrophysiol 3: 1.

Bukowski H, Lamm C (2017) Temporoparietal Junction. In: Encyclopedia of Personality and Individual Differences (Zeigler-Hill V, Shackelford TK, Eds.). Springer International Publishing, Cham, p. 1–5.

Bullmore E, Sporns O (2009) Complex brain networks: Graph theoretical analysis of structural and functional systems. Nat Rev Neurosci 10: 186–198.

Catarino A, Churches O, Baron-Cohen S, Andrade A, Ring H (2011) Atypical EEG complexity in autism spectrum conditions: A multiscale entropy analysis. Clin Neurophysiol 122: 2375–2383.

Cattell RB (1963) Theory of fluid and crystallized intelligence: A critical experiment. J Educat Psychol 54: 1–22.

Chassignolle M, Giersch A, Coull JT (2021) Evidence for visual temporal order processing below the threshold for conscious perception. Cognition 207: 104528.

Corbetta M, Shulman GL (2002) Control of goal-directed and stimulus-driven attention in the brain. Nat Rev Neurosci 3: 201–215.

Costa M, Goldberger AL, Peng CK (2002) Multiscale entropy analysis of complex physiologic time series. Phys Rev Lett 89: 068102.

Costa M, Goldberger AL, Peng CK (2005) Multiscale entropy analysis of biological signals. Phys Rev E 71: 021906.

Courtiol J, Perdikis D, Petkoski S, Müller V, Huys R, Sleimen-Malkoun R, Jirsa VK (2016) The multiscale entropy: Guidelines for use and interpretation in brain signal analysis. J Neurosci Methods 273: 175–190.

Craig JC, Busey TA (2003) The effect of motion on tactile and visual temporal order judgments. Percept Psychophys 65: 81–94.

Davis B, Christie J, Rorden C (2009) Temporal order judgments activate temporal parietal junction. J Neurosci 29: 3182–3188.

Deco G, Jirsa VK, McIntosh AR (2011) Emerging concepts for the dynamical organization of resting-state activity in the brain. Nat Rev Neurosci 12: 43–56.

Delorme A, Makeig S (2004) EEGLAB: an open source toolbox for analysis of single-trial EEG dynamics including independent component analysis. J Neurosci Methods 134: 9–21.

Der G, Deary IJ (2017) The relationship between intelligence and reaction time varies with age: Results from three representative narrow-age age cohorts at 30, 50 and 69 years. Intelligence 64: 89–97.

Dreszer J, Grochowski M, Lewandowska M, Nikadon J, Gorgol J, Bałaj B, Finc K, Duch W, Kałamała P, Chuderski A, Piotrowski T (2020) Spatiotemporal complexity patterns of resting-state bioelectrical activity explain fluid intelligence: Sex matters. Hum Brain Mapp 41: 4846–4865.

Edmonds CJ, Isaacs EB, Visscher PM, Rogers M, Lanigan J, Singhal A, Lucas A, Gringras P, Denton J, Deary IJ (2008) Inspection time and cognitive abilities in twins aged 7 to 17 years: Age-related changes, heritability and genetic covariance. Intelligence 36: 210–225.

Eramudugolla R, Irvine DRF, Mattingley JB (2007) Association between auditory and visual symptoms of unilateral spatial neglect. Neuropsychologia 45: 2631–2637.

Faisal AA, Selen LPJ, Wolpert DM (2008) Noise in the nervous system. Nat Rev Neurosci 9: 292–303.

Fernández A, Zuluaga P, Abásolo D, Gómez C, Serra A, Méndez MA, Hornero R (2012) Brain oscillatory complexity across the life span. Clin Neurophysiol 123: 2154–2162.

Fink M, Churan J, Wittmann M (2005) Assessment of auditory temporal-order thresholds – A comparison of different measurement procedures and the influences of age and gender. Restor Neurol Neurosci 23: 281–296.

Fink M, Churan J, Wittmann M (2006a) Temporal processing and context dependency of phoneme discrimination in patients with aphasia. Brain Lang 98: 1–11.

Fink M, Ulbrich P, Churan J, Wittmann M (2006b) Stimulus-dependent processing of temporal order. Behav Process 71: 344–352.

Fitzgibbons PJ, Gordon-Salant S (2004) Age effects on discrimination of timing in auditory sequences. J Acoust Soc Am 116: 1126–1134.

Fraisse P (1984) Perception and estimation of time. Ann Rev Psychol 35: 1–37.

Garrett DD, Samanez-Larkin GR, MacDonald SWS, Lindenberger U, McIntosh AR, Grady CL (2013) Moment-to-moment brain signal variability: A next frontier in human brain mapping? Neuroscience Biobehav Rev 37: 610–624.

Ghanbari Y, Bloy L, Christopher Edgar J, Blaskey L, Verma R, Roberts TPL (2015) Joint analysis of band- specific functional connectivity and signal complexity in autism. J Autism Dev Disord 45: 444–460.

Giacometti P, Perdue KL, Diamond SG (2014) Algorithm to find high density EEG scalp coordinates and analysis of their correspondence to structural and functional regions of the brain. J Neurosci Methods 229: 84–96.

Grundy JG, Anderson JAE, Bialystok E (2017) Bilinguals have more complex EEG brain signals in occipital regions than monolinguals. NeuroImage 159: 280–288.

Gu C, Liu ZX, Woltering S (2022) Electroencephalography complexity in resting and task states in adults with attention-deficit/hyperactivity disorder. Brain Commun 4: fcac054.

Helmbold N, Troche S, Rammsayer T (2007) Processing of temporal and nontemporal information as predictors of psychometric intelligence: A structural-equation-modeling approach. J Personality 75: 985–1006.

Hirsh IJ, Sherrick CE Jr (1961) Perceived order in different sense modalities. J Exp Psychol 62: 423–432.

Ho PS, Lin C, Chen GY, Liu HL, Huang CM, Lee TMC, Lee SH, Wu SC (2017) Complexity analysis of resting state fMRI signals in depressive patients. 39th Annual International Conference of the IEEE Engineering in Medicine and Biology Society (EMBC), Seogwipo.

Honey CJ, Kötter R, Breakspear M, Sporns O (2007) Network structure of cerebral cortex shapes functional connectivity on multiple time scales. Proc Natl Acad Sci 104: 10240–10245.

Honey CJ, Sporns O, Cammoun L, Gigandet X, Thiran JP, Meuli R, Hagmann P (2009) Predicting human resting-state functional connectivity from structural connectivity. Proc Nat Acad Sci 106: 2035–2040.

Jablonska K, Piotrowska M, Bednarek H, Szymaszek A, Marchewka A, Wypych M, Szelag E (2020) Maintenance *vs.* manipulation in auditory verbal working memory in the elderly: New insights based on temporal dynamics of information processing in the millisecond time range. Front Aging Neurosci 12: 194.

Jia G, Hubbard CS, Hu Z, Xu J, Dong Q, Niu H, Liu H (2023) Intrinsic brain activity is increasingly complex and develops asymmetrically during childhood and early adolescence. NeuroImage 277: 120225.

Joliot M, Ribary U, Llinás R (1994) Human oscillatory brain activity near 40 Hz coexists with cognitive temporal binding. Proc Natl Acad Sci 91: 11748–11751.

Kanabus M, Szeląg E, Rojek E, Pöppel E (2002) Temporal order judgement for auditory and visual stimuli. Acta Neurobiol Exp 62: 263–270.

Kaur Y, Weiss S, Zhou C, Fischer R, Hildebrandt A (2021) Exploring neural signal complexity as a potential link between creative thinking, intelligence, and cognitive control. J Intell 9: 59.

Kolodziejczyk I, Szelag E (2008) Auditory perception of temporal order in centenarians in comparison with young and elderly subjects. Acta Neurobiol Exp 68: 373–381.

Kosciessa JQ, Kloosterman NA, Garrett DD (2020) Standard multiscale entropy reflects neural dynamics at mismatched temporal scales: What's signal irregularity got to do with it? PLoS computational biology 16: e1007885.

Kujala T, Kallio J, Tervaniemi M, Näätänen R (2001) The mismatch negativity as an index of temporal processing in audition. Clinical Neurophysiol 112: 1712–1719.

Kumral D, Şansal F, Cesnaite E, Mahjoory K, Al E, Gaebler M, Nikulin VV, Villringer A (2020) BOLD and EEG signal variability at rest differently relate to aging in the human brain. NeuroImage 207: 116373.

Łaszewska K, Goroncy A, Weber P, Pracki T, Tafil-Klawe M (2018) Influence of the spectral quality of light on daytime alertness levels in humans. Adv Cogn Psychol 14: 192–208.

Lewandowska M, Nikadon J, Wolak T, Tołpa K, Piotrowski T, Chojnowski M, Dreszer J (2022) Resting-state fMRI functional connectivity of the left temporal parietal junction is associated with visual temporal order threshold. Sci Rep 12: 15933.

Lewandowska M, Piatkowska-Janko E, Bogorodzki P, Wolak T, Szelag E (2010) Changes in fMRI BOLD response to increasing and decreasing task difficulty during auditory perception of temporal order. Neurobiol Learn Mem 94: 382–391.

Li X, Zhu Z, Zhao W, Sun Y, Wen D, Xie Y, Liu X, Niu H, Han Y (2018) Decreased resting-state brain signal complexity in patients with mild cognitive impairment and Alzheimer's disease: a multi-scale entropy analysis. Biomed Opt Express 9: 1916.

Lin L, Chang D, Song D, Li Y, Wang Z (2022) Lower resting brain entropy is associated with stronger task activation and deactivation. NeuroImage 249: 118875.

Looney D, Adjei T, Mandic D (2018) A novel multivariate sample entropy algorithm for modeling time series synchronization. Entropy 20: 82.

Lotze M, Wittmann M, Steinbüchel N von, Pöppel E, Roenneberg T (1999) Daily rhythm of temporal resolution in the auditory system. Cortex 35: 89–100.

Luders E, Narr KL, Thompson PM, Rex DE, Jancke L, Steinmetz H, Toga AW (2004) Gender differences in cortical complexity. Nat Neurosci 7: 799–800.

Mary A, Wens V, Op de Beeck M, Leproult R, De Tiège X, Peigneux P (2017) Resting-state functional connectivity is an age-dependent predictor of motor learning abilities. Cereb Cortex 27: 4923–4932.

Mauk MD, Buonomano DV (2004) The neural basis of temporal processing. Annu Rev Neurosci 27: 307–340.

McDonough IM, Nashiro K (2014) Network complexity as a measure of information processing across resting-state networks: evidence from the Human Connectome Project. Front Hum Neurosci 8: 409.

McDonough IM, Siegel JT (2018) The relation between white matter microstructure and network complexity: Implications for processing efficiency. Front Integr Neurosci 12: 43.

McFarland DJ, Cacace AT, Setzen G (1998) Temporal-order discrimination for selected auditory and visual stimulus dimensions. J Speech Lang Hear Res 41: 300–314.

McIntosh AR, Kovacevic N, Itier RJ (2008) Increased brain signal variability accompanies lower behavioral variability in development. PLoS Computational Biol 4: e1000106.

McIntosh AR, Kovacevic N, Lippe S, Garrett D, Grady C, Jirsa V (2010) The development of a noisy brain. Arch Ital Biol 148: 323–337.

McIntosh AR, Vakorin V, Kovacevic N, Wang H, Diaconescu A, Protzner AB (2014) Spatiotemporal dependency of age-related changes in brain signal variability. Cereb Cortex 24: 1806–1817.

Micheyl C, Carlyon RP, Gutschalk A, Melcher JR, Oxenham AJ, Rauschecker JP, Tian B, Courtenay Wilson E (2007) The role of auditory cortex in the formation of auditory streams. Hearing Res 229: 116– 131.

Miskovic V, Owens M, Kuntzelman K, Gibb BE (2016) Charting moment-to-moment brain signal variability from early to late childhood. Cortex 83: 51–61.

Mizuno T, Takahashi T, Cho RY, Kikuchi M, Murata T, Takahashi K, Wada Y (2010) Assessment of EEG dynamical complexity in Alzheimer's disease using multiscale entropy. Clin Neurophysiol 121: 1438–1446.

Mognon A, Jovicich J, Bruzzone L, Buiatti M (2011) ADJUST: An automatic EEG artifact detector based on the joint use of spatial and temporal features: Automatic spatio-temporal EEG artifact detection. Psychophysiology 48: 229–240.

Noguchi Y, Kaneoke Y, Kakigi R, Tanabe HC, Sadato N (2005) Role of the superior temporal region in human visual motion perception. Cereb Cortex 15: 1592–1601.

Omidvarnia A, Zalesky A, Van De Ville D, Jackson GD, Pedersen M (2021) Temporal complexity of fMRI is reproducible and correlates with higher order cognition. NeuroImage 230: 117760.

Oron A, Szymaszek A, Szelag E (2015) Temporal information processing as a basis for auditory comprehension: clinical evidence from aphasic patients: Temporal information processing and auditory comprehension in aphasic patients. Int J Lang Commun Disord 50: 604–615.

Pahud O, Rammsayer TH, Troche SJ (2018) Elucidating the functional relationship between speed of information processing and speed-, capacity-, and memory-related aspects of psychometric intelligence. Adv Cogn Psychol 14: 3–13.

Polich J (2007) Updating P300: An integrative theory of P3a and P3b. Clin Neurophysiol 118: 2128–2148.

Power JD, Cohen AL, Nelson SM, Wig GS, Barnes KA, Church JA, Vogel AC, Laumann TO, Miezin FM, Schlaggar BL, Petersen SE (2011) Functional network organization of the human brain. Neuron 72: 665–678.

Pöppel E (1994) Temporal mechanisms in perception. Int Rev Neurobiol 37: 185–202.

Pöppel E, Bao Y, Zhou B (2011) "Temporal Windows" as logistical basis for cognitive processing. Adv Psychol Sci 19: 775–793.

Pravitha R, Srennivasan R, Nampoori VPN (2005) Complexity analysis of dense array EEG signal reveals sex difference. Int J Neurosci 115: 445–460.

R Core Team (2020) European Environment Agency https://www.eea.europa.eu/data-and-maps/indicators/oxygen-consuming-substances-in-rivers/r-development-core-team-2006. Accessed December 16, 2022.

Rammsayer TH, Brandler S (2007) Performance on temporal information processing as an index of general intelligence. Intelligence 35: 123–139.

Rey V, De Martino S, Espesser R, Habib M (2002) Temporal processing and phonological impairment in dyslexia: Effect of phoneme lengthening on order judgment of two consonants. Brain Lang 80: 576–591.

Richman JS, Moorman JR (2000) Physiological time-series analysis using approximate entropy and sample entropy. Am J Physiol Heart Circ Physiol 278: H2039–H2049.

Sabeti M, Katebi SD, Rastgar K (2015) Source localization algorithms to find attention and memory circuits in the brain. J King Saud Univ – Computer and Information Sciences 27: 334–343.

Saxe GN, Calderone D, Morales LJ (2018) Brain entropy and human intelligence: A resting-state fMRI study. PLoS One 13: e0191582.

Schütt HH, Harmeling S, Macke JH, Wichmann FA (2016) Painfree and accurate Bayesian estimation of psychometric functions for (potentially) overdispersed data. Vision Res 122: 105–123.

Seiffert AE (2003) Functional MRI studies of human visual motion perception: Texture, luminance, attention and after-effects. Cereb Cortex 13: 340–349.

Sinnett S, Juncadella M, Rafal R, Azañón E, Soto-Faraco S (2007) A dissociation between visual and auditory hemi-inattention: Evidence from temporal order judgements. Neuropsychologia 45: 552–560.

Sokunbi MO, Fung W, Sawlani V, Choppin S, Linden DEJ, Thome J (2013) Resting state fMRI entropy probes complexity of brain activity in adults with ADHD. Psychiatry Res 214: 341– 348.

Steinbüchel N von, Wittmann M, Strasburger H, Szelag E (1999) Auditory temporal-order judgement is impaired in patients with cortical lesions in posterior regions of the left hemisphere. Neurosci Lett 264: 168–171.

Swisher L, Hirsh IJ (1972) Brain damage and the ordering of two temporally successive stimuli. Neuropsychologia 10: 137–152.

Szelag E, Jablonska K, Piotrowska M, Szymaszek A, Bednarek H (2018) Spatial and spectral auditory temporal-order judgment (TOJ) tasks in elderly people are performed using different perceptual strategies. Front Psychol 9: 2557.

Szelag E, Kanabus M, Kolodziejczyk I, Kowalska J, Szuchnik J (2004) Individual differences in temporal information processing in humans. Acta Neurobiol Exp 64: 349–366.

Szelag E, Lewandowska M, Wolak T, Seniow J, Poniatowska R, Pöppel E, Szymaszek A (2014) Training in rapid auditory processing ameliorates auditory comprehension in aphasic patients: A randomized controlled pilot study. J Neurol Sci 338: 77–86.

Szymaszek A, Sereda M, Pöppel E, Szelag E (2009) Individual differences in the perception of temporal order: The effect of age and cognition. Cogn Neuropsychol 26: 135–147.

Szymaszek A, Szelag E, Sliwowska M (2006) Auditory perception of temporal order in humans: The effect of age, gender, listener practice and stimulus presentation mode. Neurosci Lett 403: 190–194.

Takahashi T, Kansaku K, Wada M, Shibuya S, Kitazawa S (2013) Neural correlates of tactile temporal- order judgment in humans: an fMRI study. Cereb Cortex 23: 1952–1964.

Tallal P, Miller SL, Bedi G, Byma G, Wang X, Nagarajan SS, Schreiner C, Jenkins WM, Merzenich MM (1996) Language comprehension in language-learning impaired children improved with acoustically modified speech. Science 271: 81–84.

Thiele JA, Richter A, Hilger K (2023) Multimodal brain signal complexity predicts human intelligence. eNeuro 10: ENEURO.0345–22.2022.

Thomas P, Rammsayer T, Schweizer K, Troche S (2015) Elucidating the functional relationship between working memory capacity and psychometric intelligence: a fixed-links modeling approach for experimental repeated-measures designs. Adv Cogn Psychol 11: 3–13.

Tononi G, Sporns O, Edelman GM (1994) A measure for brain complexity: relating functional segregation and integration in the nervous system. Proc Natl Acad Sci 91: 5033–5037.

Ulbrich P, Churan J, Fink M, Wittmann M (2009) Perception of temporal order: The effects of age, sex, and cognitive factors. Dev Cogn B Aging Neuropsychol Cogn 16: 183–202.

Vahdat S, Darainy M, Milner TE, Ostry DJ (2011) Functionally specific changes in resting-state sensorimotor networks after motor learning. J Neurosci 31: 16907–16915.

Vakorin VA (2011) Empirical and theoretical aspects of generation and transfer of information in a neuromagnetic source network. Front Syst Neurosci 5: 96.

Van Dyck D, Deconinck N, Aeby A, Baijot S, Coquelet N, Trotta N, Rovai A, Goldman S, Urbain C, Wens V, De Tiège X (2021) Resting-state functional brain connectivity is related to subsequent procedural learning skills in school-aged children. Neuroimage 240: 118368.

Wang DJJ, Jann K, Fan C, Qiao Y, Zang YF, Lu H, Yang Y (2018) Neurophysiological basis of multi- scale entropy of brain complexity and its relationship with functional connectivity. Front Neurosci 12: 352.

Wang Z (2021) The neurocognitive correlates of brain entropy estimated by resting state fMRI. NeuroImage 232: 117893.

Waschke L, Kloosterman NA, Obleser J, Garrett DD (2021) Behavior needs neural variability. Neuron 109: 751–766.

Wiener M, Hamilton R, Turkeltaub P, Matell MS, Coslett HB (2010) Fast forward: Supramarginal gyrus stimulation alters time measurement. J Cogn Neurosci 22: 23–31.

Winkler I, Brandl S, Horn F, Waldburger E, Allefeld C, Tangermann M (2014) Robust artifactual independent component classification for BCI practitioners. J Neural Eng 11: 035013.

Winkler I, Haufe S, Tangermann M (2011) Automatic Classification of Artifactual ICA-Components for artifact removal in EEG signals. Behav Brain Funct 7: 30.

Wittmann M (1999) Time perception and temporal processing levels of the brain. Chronobiol Int 16: 17–32.

Wittmann M, Szelag E (2003) Sex differences in perception of temporal order. Percept Mot Skills 96: 105–112.

Woo SH, Kim KH, Lee KM (2009) The role of the right posterior parietal cortex in temporal order judgment. Brain Cogn 69: 337–343.

Yamamoto S, Kitazawa S (2015) Tactile temporal order. Scholarpedia 10: 8249.

Zhang T, Huang W, Wu X, Sun W, Lin F, Sun H, Li J (2021) Altered complexity in resting-state fNIRS signal in autism: a multiscale entropy approach. Physiol Meas 42: 085004.

Zhang Y, Wang C, Sun C, Zhang X, Wang Y, Qi H, He F, Zhao X, Wan B, Du J, Ming D (2015) Neural complexity in patients with poststroke depression: A resting EEG study. J Affect Disord 188: 310–318.

SUPPLEMENTARY MATERIALS

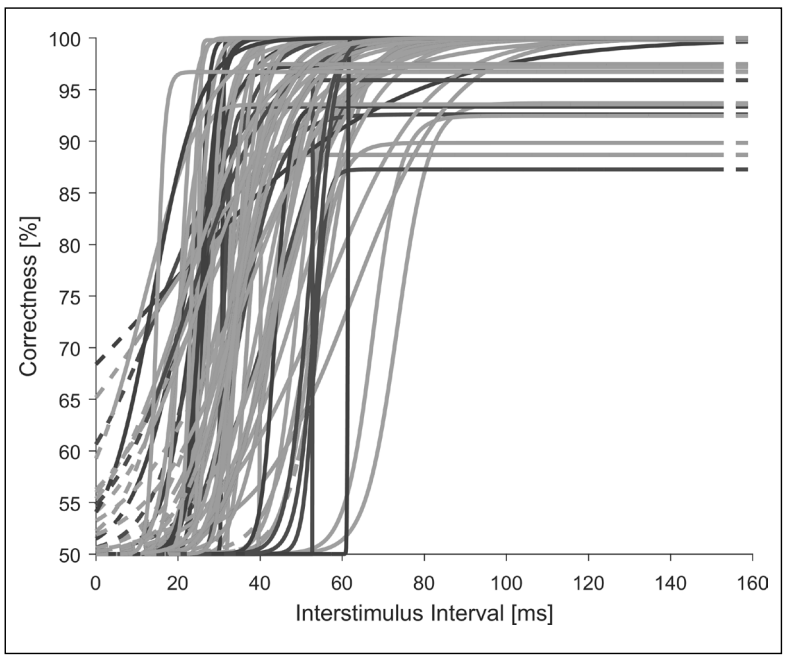

Fig. S1. Individual psychometric curves calculated from all trials of the visual Temporal Order judgment task in each subject. Since the overall correctness in the TOJ task converged to 71%, the threshold parameter of the function was set to 0.71. It is worth noting that the value of threshold of the psychometric is not equal to the temporal order threshold (TOT) value, defined as the interval for 75% correctness. Dashed line mark extrapolated ranges of the psychometric curve.

Table S1. The differences between the following three features derived from the multivariate MultiScale Entropy (mMSE) vectors: AUC, MaxSlope and AvgEnt, calculated for central (CE), left anterior (LA), left middle (LM), left posterior (LP), right anterior (RA), right middle (RM) and right posterior (RP) channel sets. The down and up arrows indicate the direction of significant ($P< 0.05$) differences between the areas placed in the columns (I) and rows (J) (mean difference, I-J). A lack of significant differences between particular areas are marked with "–". CE – central, LA – left anterior, LM – left middle, LP – left posterior, RA – right anterior, RM – right middle, RP – right posterior.

Mean difference (I-J)		I	CE			LA			LM			LP			RA			RM			RP		
			AUC	MaxSlope	AvgEnt	AUC	MaxSlope	AvgEnt	AUC	MaxSlope	AvgEnt	AUC	MaxSlope	AvgEnt	AUC	MaxSlope	AvgEnt	AUC	MaxSlope	AvgEnt	AUC	MaxSlope	AvgEnt
J	CE					↓	↓	↓	↓	↓	↓	↓	↓	↓	↓	↓	↓	–	↑	–	↓	↓	↓
	LA		↑	↑	↑				↑	↑	↑	↑	↑	–	–	–	–	↑	↑	↑	↓	–	↓
	LM		↑	↑	↑	↓	↓	↓				↓	↓	↓	↓	↓	↓	↑	↑	↑	↓	↓	↓
	LP		↑	↑	↑	↓	↓	–	↑	↑	↑				↓	↓	–	↑	↑	↑	↓	↓	↓
	RA		↑	↑	↑	–	–	–	↑	↑	↑	↑	↑	–				↑	↑	↑	↓	–	↓
	RM		–	↓	–	↓	↓	↓	↓	↓	↓	↓	↓	↓	↓	↓	↓				↓	↓	↓
	RP		↑	↑	↑	↑	↑	↑	↑	↑	↑	↑	↑	↑	↑	–	↑	↑	↑	↑			

Table S2. The results of correlation analysis between age and the three features (AUC, MaxSlope and AvgEnt), derived from the multivariate MultiScale Entropy (mMSE) vectors, calculated for the central (CE), left anterior (LA), left middle (LM), left posterior (LP), right anterior (RA), right middle (RM) and right posterior (RP) channel sets. The "**" symbol represents $P<0.01$, whereas the "*" symbol indicates $P<0.05$. The r represents the Pearson's correlation coefficients and FDR – False Discovery Rate.

Variable		*r*	*P* value (uncorrected)	*P* value (FDR corrected)
AUC	CE	-0.171	0.155	0.686
	LA	-0.064	0.594	0.849
	LM	-0.098	0.418	0.836
	LP	-0.101	0.400	0.836
	RA	-0.047	0.695	0.849
	RM	-0.134	0.266	0.766
	RP	-0.033	0.785	0.863
MaxSlope	CE	-0.058	0.630	0.849
	LA	-0.039	0.749	0.863
	LM	-0.048	0.693	0.849
	LP	-0.056	0.645	0.849
	RA	0.010	0.935	0.979
	RM	-0.074	0.541	0.849
	RP	-0.002	0.985	0.985
AvgEnt	CE	-0.308	0.01**	0.2
	LA	-0.127	0.291	0.766
	LM	-0.217	0.069	0.505
	LP	-0.170	0.156	0.686
	RA	-0.121	0.313	0.766
	RM	-0.253	0.034*	0.369
	RP	-0.086	0.475	0.849